

VIP Very Important Paper

Mechanistic Insights of Photocatalytic CO₂ Reduction: Experimental versus Computational Studies

Anna M. Masdeu-Bultó,^[a] Mar Reguero,^{*[a]} and Carmen Claver^{*[a]}

To stop the global warming, a complementary alternative to the decrease of CO₂ production is the reduction of its amount in the atmosphere by capture and transformation into consumer products. One of the most interesting primary products is CO, used to synthesise liquid fuels. Perhaps the most attractive way of reducing CO₂ to CO is the photocatalytic route. To know the details of the mechanism of this reaction can help in the

design of more efficient catalytic systems. In this review, we compile the studies, undertaken from both computational and experimental approaches, of the reaction mechanism of the photoreduction of CO₂ to CO by molecular catalytic systems based on transition metal complexes. The combination of experimental and computational studies can be crucial to achieve the goal aimed.

1. Introduction

The energy demand is continually growing due to the rapid growth of the world's population together with the increasing level of industrialisation and development. Nowadays energy production comes mainly from fossil fuels with the consequent production of carbon dioxide (CO₂) and the well-known problems that it entails. In 2019 fossil fuels still supplied 84% of the world's energy consumption.^[1] In addition, fossil fuels are the main source of raw materials for plastics, fertilisers, chemicals, and pharmaceuticals.

Anthropogenic CO₂ emissions are estimated at 35 Gt per year. This amount cannot be absorbed by the plant's photosynthesis and has led to a concentration of above 400 ppm of CO₂ in the atmosphere.^[2] Being CO₂ one of the gases that generate the greenhouse effect, the increase in its concentration is considered to contribute to climate change, which is reflected, for example, in the rise of the global temperature of the planet. Recent climate summits (Kyoto 1992, Paris 2015 and Chile-Madrid 2019 and the Glasgow Climate Change conference 2021) have concluded that carbon dioxide emissions should be reduced by 45% by 2030 and reach a net-zero by 2050 to limit global warming to 1.5 °C.^[3] Achieving this objective requires a combination of efforts in different areas. Reducing the use of fossil fuels by renewable energy sources and replacing them with other fuels (such as hydrogen) are the ways to avoid CO₂ production. In the last years, there has been a great develop-

ment in the use of renewable energies such as hydro, wind or solar, although they still present problems due to their intermittency and the challenge of their storage, which makes them still difficult to incorporate in the energy system.

In July 2020 the European Union (EU) set out a plan to eliminate by 2050 net greenhouse gas emissions, including CO₂, to achieve a climate-neutral society.^[4] Within the same EU plan, the "hydrogen strategy" was adopted, which aims to use clean hydrogen generated by the electrolysis of water as the major fuel for 2030.^[4,5]

Moreover, the World Energy Outlook 2020 considers the energy sector globally to reach Net Zero Emissions by 2050 (NZE2050) identifying the targets which are included in the Sustainable Development Scenario (SDS).^[6]

Even if avoiding CO₂ production is the main requirement and challenge for the social development in our near future, the complementary alternative of reducing the CO₂ emissions into the atmosphere through its capture and storage (CCS) and its utilisation into consumer products (CCU) also plays an important role in this scenery.^[7,8] Several CO₂ capture procedures are already being used.^[9,10] The research and development of the CCS technologies which should be different depending on the CO₂ sources are receiving continuous impulse due to their intrinsic interest, but they still need to improve efficiency to contribute to the achievement of the 2050 objectives.^[11] For the CCU, given that CO₂ is a very stable molecule ($\Delta G_f^0 = -394.228 \text{ kJ/mol}$)^[12] the transformation of CO₂ into other products needs the use of catalysts and/or other highly reactive substances. The important advances in this strategy during the last decades, developed with the increased support of research agencies as well as industrials and scientific institutions, have been remarkable.^[13] Chemical-, photo- and electrocatalysis mainly with the use of transition metal catalysts, offer ways to transform CO₂ in hydrocarbon fuels^[14-16] and valuable chemicals.^[17-24] These catalytic processes constitute powerful, profitable and attractive strategies since carbon dioxide is a low-cost and abundant carbon source for all carbon-based materials.

[a] Prof. A. M. Masdeu-Bultó, Prof. M. Reguero, Prof. C. Claver
Department of Physical and Inorganic Chemistry
Universitat Rovira i Virgili
Carrer Marcel·lí Domingo, 1, Campus Sescelades, 43007 Tarragona, Spain
E-mail: mar.reguero@urv.cat
carmen.claver@urv.cat
http://www.quimica.urv.es/w3qf/

Part of the "RSEQ-GEQO Prize Winners" Special Collection.

© 2022 The Authors. European Journal of Inorganic Chemistry published by Wiley-VCH GmbH. This is an open access article under the terms of the Creative Commons Attribution Non-Commercial License, which permits use, distribution and reproduction in any medium, provided the original work is properly cited and is not used for commercial purposes.

Concerning the structural and electronic characteristics of CO₂, it is a linear, apolar molecule with C–O bond distances of 1.16 Å. Its HOMO (highest molecular occupied orbital) is a doubly occupied 1Π_g orbital, located mainly on the oxygen atoms, while the LUMO (lowest unoccupied molecular orbital) is a 2Π_u centred primarily on central carbon.^[25] This gives a nucleophilic character to oxygens and an electrophilic nature to carbon, making CO₂ an amphoteric oxide in which oxygens exhibit Lewis base character while carbon can play the role of an acidic centre. However, CO₂ is a better acceptor than electron donor since the behaviour of the molecule is dominated by the characteristics of the central carbon. In fact, the proton affinity of CO₂ oxygens is only about 129.2 kcal mol⁻¹, quite lower than that of water, for example, while its ionisation potential is high, 318.2 kcal mol⁻¹. The transfer of electrons to the LUMO increases the C–O distance while inducing a loss of linearity in the molecule.^[25]

The activation of CO₂ in catalytic processes often occurs by coordination with a metal centre that can be produced in different ways (Figure 1):

- η¹-OCO “end-on” coordination occurs through the HOMO 1Π_g electron pair centred on the terminal oxygens. CO₂ maintains a linear geometry which indicates that there is no retro-donation to level 2Π_u. This coordination is very rare.^[26]
- η¹-CO₂ coordination where the d electrons of the metal are transferred to LUMO 2Π_u of the CO₂ located mainly on the carbon atom. In this mode of coordination, the CO₂ molecule

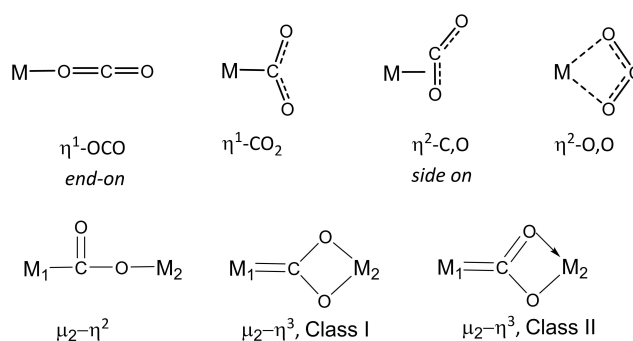


Figure 1. Possible ways of CO₂ coordination to metal centres.

loses its linearity, and the nucleophilic character of the oxygens is modified. In many cases, this coordination occurs assisted by a second metal core.^[27]

- η²-C,O “side on” coordination. This mode is very common. It can be explained by the formation of a bond by donation of the electrons centred on the atom of O (1Π_g and 1Π_u) and a significant backdonation of d electrons from the metal to the LUMO 2Π_u centred on the C, what increases the oxidation state of the metal. This coordination shows up the amphoteric character of CO₂.^[25]



Carmen Claver is Professor of Inorganic Chemistry at the Rovira i Virgili University (URV) of Tarragona since 1991 and Emeritus Professor from 2020. Her research focuses on sustainable aspects of catalysis: selectivity through catalyst design, recycling of supported homogeneous catalysts, nanocatalysts, and development of efficient catalysis for CO₂ and biomass transformation. Research leader from 1985, Vice-Rector of Research URV (1993–1997) Scientific Director of the “Technological Centre of Chemistry of Catalonia” and Director of the “Unit of Technology Chemistry” Eurecat from 2009 until 2020. Recognised as Distinguished Researcher by the Catalan Government (2003), Distinguished Professor URV (2004), Medal “Narcís Monturiol” (2007) Catalan Government and Correspondent member of the Royal Academy of Sciences of Spain (2010). Chair of excellence Pierre de Fermat in Toulouse, France (2009–2011), member of the Scientific Council of the National Council of Scientific Research (CNRS) France (2009–2014). Member of the Academia Europea (2012), “Ciamician-Gonzalez” Lecturer Award by “Real Sociedad Española de Química” (RSEQ) and “Società Chimica Italiana” (SCI) (2014) Gold Medal for Research Organometallic GEQO (2015) ‘Miguel Catalán-Paul Sabatier’ Price, Société Chimie Française (2016) Doctor “Honoris Causa”, University Paul Sabatier, Toulouse (2019).



Anna Masdeu-Bultó is Professor of Inorganic Chemistry at the Department of Physical and Inorganic Chemistry (University Rovira i Virgili, Tarragona, Spain) since 2020. She obtained the PhD in Chemical Sciences (1992) at the University of Barcelona (Faculty of Chemistry of Tarragona) working on rhodium catalysed hydroformylation under Professor Carmen Claver and Aurora Ruiz guidance and pursued postdoctoral research at Ottawa University in Prof. Howard Alper’s group (1992). Her research interest has been focused on different aspects of catalysis such as the use of green solvents and carbon dioxide transformation.



Mar Reguero is Professor of Physical Chemistry at the Department of Physical and Inorganic Chemistry of the Universitat Rovira i Virgili (URV at Tarragona, Spain). She studied at the Universidad Complutense of Madrid, obtaining her PhD in Chemical Sciences in 1989. She then worked as a postdoctoral researcher at King’s College London, UK (1990), at the Spanish Research Council, Madrid (1991) and for Daresbury Laboratory, UK (1992). In 1993 she moved to the Department of Physical and Inorganic Chemistry of the Universitat Rovira i Virgili (URV at Tarragona, Spain), where she is Professor since 2021. Her research in the Chemistry field, as a member of the Quantum Chemistry group of URV, is focused on the computational elucidation of mechanisms of photochemical and catalytic reactions.

– η^2 -O,O coordination. This one, by donation of electrons centred on the oxygen atoms, has not been observed often, and mainly with group 2 metals.^[25]

In general, the interaction with electron-rich species (nucleophiles such as metals in low oxidation state, bases, etc.) is more likely through the carbon atom, while when it comes to electron-poor centres (electrophiles such as metals in high oxidation states) the interaction usually occurs through the oxygen atoms.

Coordination of CO₂ with several metal centres (μ_2 - η^2 , μ_2 - η^3), is also possible. The most common bonding modes in dinuclear complexes are also shown in Figure 1.

When coordination takes place through C, the CO₂ reduction can be favoured by the interaction of a Lewis acid with the oxygen atoms. This bifunctional activation highlights the importance of the interactions in which a donation of electrons and protons can occur simultaneously to produce a proton-coupled electron transfer (PCET). Multielectronic reduction of CO₂ can result in several products of interest, as shown in Table 1. This table shows that most reactions occur in the presence of protons and that, apart from the reduction reaction to the radical CO₂^{•-}, all their reduction potentials are very similar. For this reason, all these reactions are competitive with each other and with the hydrogen production reaction ($2\text{H}^+ + 2\text{e}^- \rightarrow \text{H}_2$; $E^0 = -0.41$ V), and the pre-eminence of one reaction over the others may depend on several factors like the catalyst, the presence of water or other reactants or the pH of the reaction medium. The complex influence of these factors makes selectivity an important issue in the reductive transformation of CO₂.^[28]

Among the possible products of reduction of CO₂, CO is especially interesting for being one of the intermediates used to synthesise liquid fuels by the classic reductive dihydrogenation process of Fischer–Tropsch.^[29,30]

In any case, given the great thermodynamic stability of CO₂, an energy contribution is needed for its transformation. There are different ways to achieve it such as thermal,^[31] electrochemical^[32] photochemical^[33,34] or biochemical^[35,36] processes, all of them under intense research.

The photochemical route is one of the most attractive and promising, and on which this review focuses. The sun provides in just two hours the energy that humanity consumes in a year,^[37] making this clean and renewable energy the most sustainable and accessible. Its use for the fixation and trans-

formation of CO₂ is a process that mimics natural photosynthesis and does not generate primary or secondary pollution.^[38] If this transformation produces any of the so-called “solar fuels”, the carbon cycle is closed, also relieving the problem of the energy crisis and global warming from two different fronts. In fact, one of the most studied strategies in recent years for obtaining solar fuels is the development of catalysts capable of using solar radiation directly (photoactive systems) or indirectly (by cooperation with a photosensitiser) to generate hydrogen (H₂) or CO₂ reduction products, which is known as artificial photosynthesis.^[28,39–41]

In this scenario and considering the impact that photocatalytic reduction of CO₂ can have in fuels and chemicals production, it is evident that the detailed knowledge of the mechanism of these reduction processes could help in the design of better catalytic systems to enhance the efficiency of the catalytic transformations of CO₂. Traditionally, experimental evidence has been the source of information that researchers have used to propose reaction mechanisms. Computational results were, a few decades ago, only a punctual help for this endeavour, but the development of computational methods and computing power have made this resource another usual tool. Nowadays it is useful not only to corroborate experimental hypotheses or “predict the past”, but it can already be also used for predictive purposes. The more and more accurate computation of energy profiles of reaction paths allows to picture detailed reaction mechanisms, but the complexity of the photocatalytic reduction of CO₂ and the large number of alternative reaction paths that should be explored make this study a difficult challenge for computational chemistry.

To have a clearer view of the state of the art in these types of studies and gain a deeper understanding of the mechanisms of CO₂ photoreduction by molecular catalysts, we analyse here the individual studies performed both at computational and experimental level, relating the proposal based on computational calculations with the evidence of the mechanism obtained from experimental electrochemical and spectroscopic studies, to draw a global picture of the possible mechanisms of this reaction and to highlight the synergy between these complementary approaches.

Previous to this, in the next section, we will present general aspects of the CO₂ reduction with molecular catalysts and the general reaction mechanisms proposed from both computational calculations and experimental evidence. Next, we will describe the most common catalytic system used for photochemical reduction of CO₂ and comment on their global performance. In the following section, we compile the works that include computational studies to determine reaction mechanisms. Finally, we summarise and present the conclusions of this compilation in the last section of this paper.

Table 1. Some of the products of CO₂ reduction and aqueous medium reduction potentials using the normal hydrogen electrode (NHE) as a reference.^[42]

Semi-reaction reduction	E^0 [V]
$\text{CO}_2 + 0 \text{H}^+ + 1 \text{e}^- \rightarrow \text{CO}_2^{\square-}$	-1.93
$2\text{CO}_2 + 0 \text{H}^+ + 2 \text{e}^- \rightarrow \text{C}_2\text{O}_4^{2-}$	-0.59
$\text{CO}_2 + 0 \text{H}^+ + 2 \text{e}^- \rightarrow \text{HCOO}^-$	-0.39
$\text{CO}_2 + 2 \text{H}^+ + 2 \text{e}^- \rightarrow \text{HCOOH}$	-0.61
$\text{CO}_2 + 2 \text{H}^+ + 2 \text{e}^- \rightarrow \text{CO} + 1 \text{H}_2\text{O}$	-0.53
$\text{CO}_2 + 4 \text{H}^+ + 4 \text{e}^- \rightarrow \text{HCHO} + 1 \text{H}_2\text{O}$	-0.48
$\text{CO}_2 + 6 \text{H}^+ + 6 \text{e}^- \rightarrow \text{CH}_3\text{OH} + 1 \text{H}_2\text{O}$	-0.38
$\text{CO}_2 + 8 \text{H}^+ + 8 \text{e}^- \rightarrow \text{CH}_4 + 2 \text{H}_2\text{O}$	-0.24

2. Generic mechanism of the CO₂ reduction reaction using molecular catalysts

Sticking to molecular catalysts formed by complexes of transition metals (the most used as homogeneous catalysts), a good amount of generic information on the mechanisms of the reaction of CO₂ reduction has already been reported. For the reaction to take place, four events must occur: absorption of photons by a photoactive species, separation of charges (or generation of hollow-electron pairs), transfer of electrons to the catalyst and finally transformation from the substrate to the product with the cooperation, in most cases, of an agent that provides protons. For these stages to occur, most photocatalytic CO₂ reduction systems consist of a sacrificial electron donor (SD), a photosensitiser (PS) that absorbs radiation and acts as a mediator in the electron transfer, and the molecular catalyst (Cat) that activates CO₂ and induces the reduction reaction.^[28]

When the photosensitiser PS absorbs radiation, it is promoted to an excited state (PS*) whose characteristics can be very different from those of the ground state, so it can lead to processes that can be unviable in its most stable state. Among other things, its ionisation potential and electron affinity are lower than in the ground state, making PS* a better oxidant and reductive species than PS. But for the excited species to give rise to other events, its lifetime cannot be extremely short. For this reason, in photosensitisers, it should be possible to populate an excited triplet state through an effective intersystem crossing (ISC) that transfers the population from the singlet state directly reached by the photon absorption to a triplet state with a long lifetime. From this triplet state, several phenomena like energy transfer or reductive or oxidative quenching deactivations can occur, as outlined in Scheme 1

If the PS* is a strong enough oxidant, the reductive deactivation Scheme 1a) will take place. PS* will oxidise the SD in a reducing deactivation (Scheme 1a) forming the reduced species of the PS (PS⁻), which will be a reductant stronger than the PS and the PS*. For the species PS⁻ to reduce the catalyst, the redox potential of the first must be smaller than that of the second. The PS⁻ is then oxidised to return to its ground state reducing the catalyst. The reduced catalyst will then be the species responsible for the reduction of CO₂.

On the other hand, in the oxidising deactivation (Scheme 1b), the PS* must be a strong enough reductant, so the

oxidation of the PS* and the concomitant reduction of the catalyst occur first. The reduced catalyst will then be able to reduce CO₂. The oxidised PS (PS⁺) will be restored to its ground state by reduction at the expense of the SD.

In the event of an energy transfer to the catalyst, the PS will return to its ground state while the catalyst will be excited to a triplet state (³Cat*), preserving the system's overall spin angular momentum. For this energy transfer to be possible, the excitation energy of the PS* must be greater than that of the ³Cat*. The excited state of the catalyst will be (for the same reasons as those applied to the case of PS*), a stronger oxidant than its ground state, so it will be reduced by oxidising the SD and then will be able to reduce CO₂.

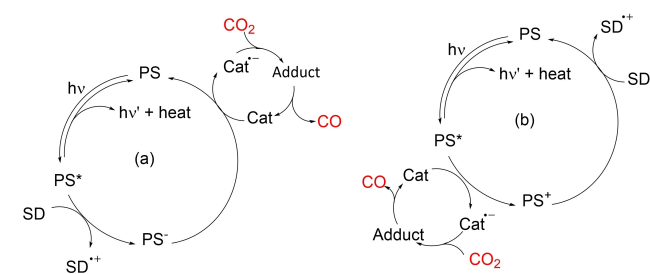
But to obtain CO, a double reduction of CO₂ must occur, so the catalyst must accept at least two electrons in consecutive redox processes, interacting repeatedly with the PS, the SD, or with products of the evolution of the oxidised SD, which are sometimes also the source of the two protons necessary for the reaction. These protons can also come from H₂O present in the reaction medium, but under these conditions, the importance of the selectivity problem increases since the reaction of H₂ formation enters into competition.

The interaction between CO₂ and the molecular catalyst usually occurs either by the insertion of CO₂ into a metal-hydride bond or by bonding to a vacancy of the coordination sphere of the metal centre. In the first case, electrostatic attractions occur between the C–O and M–H bonds, both polarised, placing the carbon of CO₂, which is the electrophilic centre, close to the nucleophilic hydride. On the other hand, when CO₂ occupies a vacant coordination position, a η¹-CO₂ type interaction occurs, so the oxygens are placed in a position that favours their protonation. In general, the first type of interaction results in formic acid while the second is more frequent in obtaining CO. In fact, all the computational studies about reduction of CO₂ to CO of which we are aware, find an interaction of η¹-CO₂ type between the metal of the catalyst and CO₂. The mechanisms suggested for the different catalysts studied differ mainly in the order in which the different stages of the reaction are proposed to take place.^[42]

In general, it is assumed that the stage corresponding to the second electron transfer and rupture of the C–OH bond is the limiting stage of the reaction rate and therefore, the more easily the OH is eliminated, the faster the conversion of CO₂ to CO will be.^[43] Compared with this stage, the removal of CO is considered simple,^[44,45] although with some catalysts the dissociation of CO does not occur easily and the carbonyl species inhibits the catalysis.^[46]

Mechanistic studies also indicate that the capacity of the substrate to establish a double coordination can stabilise certain intermediates of the reaction, which would favour the obtention of CO. This would explain the significantly better activity of certain bimetallic complexes compared to analogous systems with a single metal centre.^[44,47,48]

Nevertheless, there are still many unknowns concerning the mechanisms of these reactions, and there are many different reaction paths for the different reaction systems analysed as the following revision will show up.



Scheme 1. Two of the possible mechanisms of deactivation of the photosensitiser: (a) by reducing deactivation and (b) by oxidising deactivation.^[28]

3. General description of molecular catalytic systems used for the reduction of CO₂ to CO

The first published work on the selective photoreduction of CO₂ to CO using a molecular catalytic system is due to Lehn's group, who in 1983 proposed a Re(I) catalysts for this purpose.^[49] The complexes *fac*-[Re(**bpy**)(CO)₃(X)] (**bpy** = 2,2'-bipyridine; X = Cl, Br) (1, Scheme 2) acted as photosensitiser and catalyst for the reduction of CO₂ to CO selectively. In the presence of an excess of Cl⁻ ions, *fac*-[Re(**bpy**)(CO)₃Cl] produced CO with a quantum yield of 14% and a faradaic efficiency of 98% and consumed a tertiary amine, triethanolamine (TEOA, Figure 4), as electron donor species in dimethylformamide.^[49,50] The catalytic mechanism proposed is represented in Scheme 2.

Since then a good number of catalysts based on Re and other precious metals such as Ru(II) or Ir(III) have been proposed (recent works on this subject can be found for Re,^[51–56] Ru,^[57,58] Ir,^[59] and, although less frequently, also for Rh, Os, Pd or Mo^[60,61]).

The high price of these metals has led to the search, in the last decade, for catalysts based on the more earth-abundant metals of the first transition period (3d metals), which essentially are those found in the biological catalysts that carry out the reduction of CO₂.^[39] But replacing 4d and 5d by 3d metals does not only have economic advantages, as some notable differences between them add other good reasons for the use of the latter. For example, Fe(II) and Ni(II) tend to rapid exchange of ligands, while their corresponding analogues of the 4d and 5d periods are usually more inert, slowing down or even preventing the coordination of the substrate or the dissociation of the product, which produces deactivation of the catalyst.^[42]

The most commonly used 3d metals so far have probably been Co,^[44–46,62–65] Ni,^[66–69] and Fe,^[70–73] while Mn,^[74,75] and Cu^[76,77] have been less studied.

The main classes of ligands used in molecular catalysts of metal complexes are nitrogen-donors of polypyridyl kind such as 2,2'-bipyridine (**bpy**) or 2,2':6',2''-terpyridine (**tpy**), 1,4,8,11-tetraazacyclotetradecane (**cyclam**) derivatives, porphyrins,

phthalocyanines and related aza-macrocycles (Figure 2). The most common ligands are polypyridyls since they are easily modifiable, give rise to more soluble complexes in water or polar solvents and can be readily immobilised to obtain heterogeneous catalysts. These ligands are also found in combination with carbonyl or halogen ligands.^[78] It is also common to find complexes with a coordination position occupied by a labile solvent molecule that can be readily exchanged by the carbon dioxide substrate.^[63,76,79,80]

Another component of the catalytic systems for CO₂ reduction that have a great influence on the effectiveness of the reaction is the photosensitiser. Its absorption spectra, lifetime of excited states, photostability and redox properties directly affect the activity and selectivity of the process. Despite all the progress made to avoid precious metals in catalysts, most PS are still Ru or Ir complexes. The most studied and used ones are [Ru(**bpy**)₃]²⁺ (**PS1**, Figure 3)^[81] and [Ir(**ppy**)₃] (**PS2**, Figure 3).^[82] Both have the advantages of exhibiting wide absorption bands in the visible region and having triplet states of long half-life times and, although in their ground state they

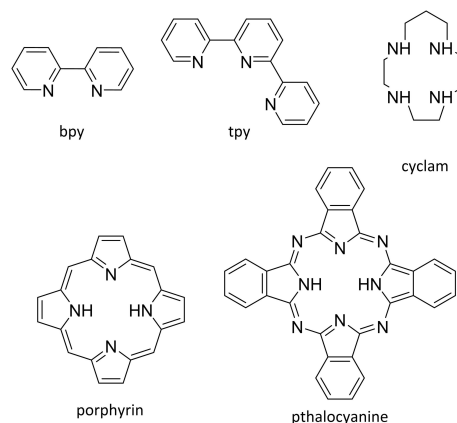
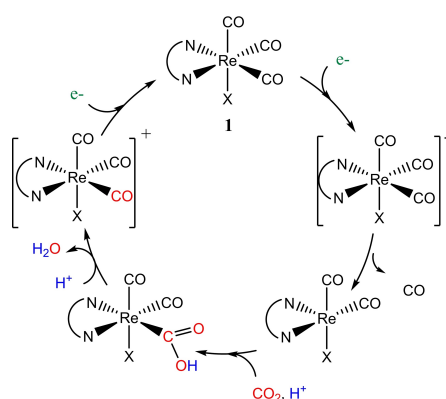


Figure 2. Main classes of ligand types used in molecular catalysts of metal complexes for the photoreduction of CO₂. **bpy** = 2,2'-bipyridine, **tpy** = 2,2':6',2''-terpyridine, **cyclam** = 1,4,8,11-tetraazacyclotetradecane.



Scheme 2. Proposed possible mechanism for the Re-catalysed reduction of CO₂ to CO. Adapted from Lehn and co-workers.^[49,50]

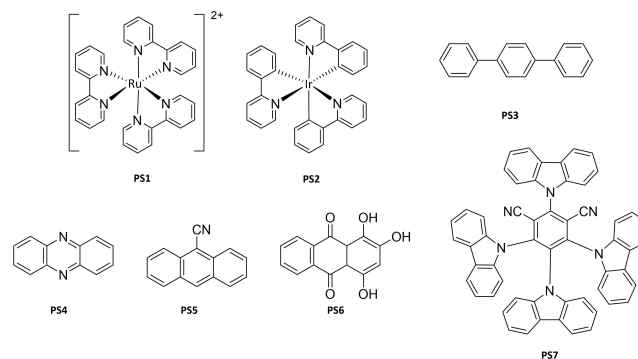


Figure 3. Structure of the most common photosensitisers: **PS1** = [Ru(**bpy**)₃]²⁺ and (**bpy** = 2,2'-bipyridine), **PS2** = [Ir(**ppy**)₃] (**ppy** = 2-phenylpyridine), **PS3** = *p*-terphenyl, **PS4** = phenazine, **PS5** = 9-cianoanthracene, **PS6** = purpurine, **PS7** = 1,2,3,5-tetrakis(carbazol-9-yl)-4,6-dicyanobenzene.

are poor reductants and poor oxidants, in their excited states they become powerful and versatile electron transfer agents.^[83]

Recently, Cu and Zn complexes have begun to be used as photosensitisers, gradually improving their selectivity, efficiency and robustness.^[84–86] Another alternative is the use of organic pigments, such as *p*-terphenyl, phenazine, 9-cyanoanthracene, purpurine (**PS3–PS6**, Figure 3)^[78,84] However, these PSs are not free of problems, such as the need for ultraviolet light to be excited,^[87] since the absorption of visible light is limited to rare exceptions like **PS7**.^[88–90] It is interesting to note that the use of phenazine as PS leads to the formation of formic acid as the major product instead of CO^[91] which demonstrates the critical and determining role that the PS has in the catalytic reaction.

In all the cases collected in this review the reactions were induced using visible light.

The last component of catalytic CO₂ photoreduction systems, the sacrificial electron donor, has less variation in the studies run so far (most common ones shown in Figure 4). Ascorbic acid and triethanolamine are the most commonly used, especially in the aqueous medium, but triethylamine (TEA) and 1,3-dimethyl-2-phenyl-2,3-dihydro-1H-benzo[d]-imidazole (BIH) are also often used.^[87] In some works it is proposed that amines (TEA and TEOA) are also a source of protons, resulting in α -amino radicals in their decomposition.^[48,62]

In a short time, much progress has been made in the efficiency of these catalysts. In the last decade, most catalytic systems reached values of the turnover number (TON) of the order of 10⁻¹ to 10³ and of the turnover frequency (TOF) from 10⁻⁵ to 10⁻¹ s⁻¹, but some systems appeared later that broke these barriers, reaching even higher values of TON and TOF. For instance, for the Ni(II) complex [Ni(**bimiq**)(NCCH₃)](PF₆)₂ (**2**, Figure 5) with a N-heterocyclic carbene-amine ligand, bis(3-

(imidazole)isoquinoliny)-propane (**bimiq**), 98000 TON and 3.9 s⁻¹ TOF were reported using an acetonitrile solution of **PS1** (Figure 3) as photosensitiser and TEA as sacrificial reductant.^[67] Another high-performance catalyst is the Co(II) complex [Co(**tpea**)(NCCH₃)](ClO₄)₂ (**3**, Figure 5) containing the polyodal ligand tris[2-(iso-propylamino)ethyl]amine (**tpea**) which showed a high TON of 44800 and a TOF of 1.24 s⁻¹.^[79] However, these are exceptional cases that stand out from the whole, since most catalysts show relatively low efficiencies and selectivities, which decrease in systems where water is present due to the competition with the proton reduction reaction.

A very promising option is presented by complexes with more than one metal centre, which show higher catalytic activities than their monometallic analogues. The reason for that was attributed to the ability they have to activate CO₂ by joint coordination to the two metal centres.^[44,47,92] For example, in the case of the cryptate dinuclear complex [Co₂(OH)(**crypt**)](ClO₄)₃ (**crypt** = N[(CH₂)₂NHCH₂(*m*-C₆H₄)CH₂NH-(CH₂)₂]₃N, **4**, Figure 5) the TON is more than 5 times greater per Co atom than that of its analogue with a single cobalt centre [Co{N[(CH₂)₂NHCH₂(C₆H₅)₃(NCCH₃)](ClO₄)₂} (**6**, Figure 5). Moreover, the heterobimetallic analogue **5** (Figure 5) showed higher photocatalytic activity and selectivity for CO₂ reduction than the corresponding dinuclear homometallic and mononuclear complexes.^[47] Similarly, an increase of activity was obtained using the pentanuclear complex [Co₅(**btz**)₆(NO₃)₄(H₂O)₄] (**btz** = benzotriazolate), although mixtures of CO and H₂ were obtained.^[92]

The possibility of a double activation of CO₂ can also be achieved in monometallic complexes with certain ligand architectures that allow two *cis* positions of coordination for CO₂, such as *cis*-[Co(**pdp**)Cl₂] (**pdp** = 1,1'-bis(2-pyridinylmethyl)-2,2'-bipyrrolidin, **7**, Figure 5) with which a TON of 368 was obtained.^[62]

An interesting option would be the use of catalysts that could directly absorb radiation to be activated and then oxidise the sacrificial donor and reduce CO₂, but few efficient examples are known so far, and some have problems of selectivity or robustness. Noteworthy exceptions are some Fe complexes with porphyrin derivatives^[93,94] with which high selectivity was obtained. In fact, modified tetraphenylporphyrins, mainly that with trimethylammonium groups at the *para* position of each phenyl ring, show to overcome many of the mentioned problems. This catalyst acts without the need of PS and, with BIH as SD, yields a TON value of 101 after long continuous irradiation, demonstrating the robustness of the catalyst, and with a 100% of selectivity towards CO formation even in acid solutions.^[93]

4. Mechanistic studies of catalytic photoreduction of CO₂

Mechanistic studies of the CO₂ photocatalytic reduction generally involve the elucidation of the mechanism of photo-excitation of the photosensitiser, the determination of the

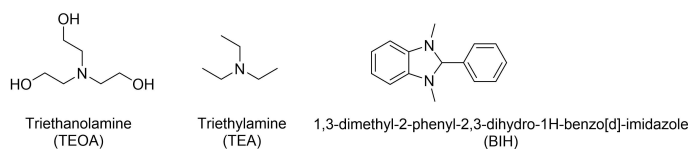


Figure 4. Structure of the most common sacrificial donors.

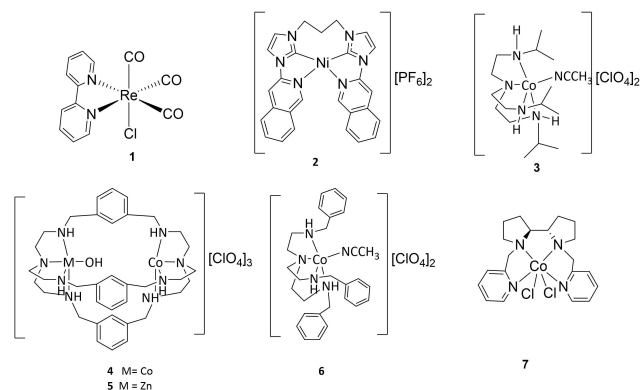


Figure 5. Some molecular catalysts for photoreduction of CO₂.

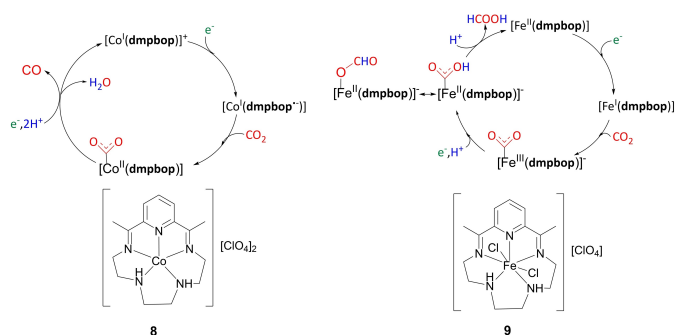
nature of the CO₂ activation and the identification of the elementary processes and species formed in the electron-proton transfer steps in which catalyst, sacrificial electron donor and photosensitiser participate.

For molecular-based catalysts, the proton-electron transfer sequences and breaking of C–O bonds are analysed experimentally by cyclic voltammetry (CV)^[95,96] together with spectroscopic techniques (UV-vis, FT-IR, EXAFS and NMR) to identify the structure of intermediate species of the mechanistic cycle.^[46] Fluorescence quenching experiments allow determining the parameters related to the electron transfer process between the excited photosensitiser and the catalyst.^[97]

Computational studies of photocatalytic reactions did not begin until relatively a few years ago, with no publications found before 2013. For the particular case of the mechanisms of catalytic photoreduction reactions from CO₂ to CO using molecular transition metal-based catalysts, the first studies are even more recent (2015) and globally they are not very abundant. All of them use methods based on the density functional theory (DFT) and the most used functionals are the B3LYP,^[62,80,96,98] in most cases^[46,48,80,92] with the D3 correction for the dispersion proposed by Grimme,^[99] and the M06 in some of its variants (M06L, M06-2X, M06-D3).^[47,56,62] In general the geometries are optimised in the gas phase with a more modest basis set (they use usually pseudopotential for metals and 6–31G(d) for the rest of the atoms), and the energies are refined including the effect of the solvent with the Polarizable Continuum Model (PCM) or Solvent Model Density (SMD) using somewhat larger bases (the pseudopotential for the metal is maintained and the bases of the rest of the atoms are extended in many cases to 6–311 + G(d)).

Although in some cases only some parameters of the reactive species,^[63,100] relative energies of possible intermediates,^[101,102] or some specific energy barriers (free energies of transition states)^[45] are calculated to elucidate the mechanism of the reaction, in most cases, the energy profile of the different stages of the reaction, beginning from the reduced catalyst, is determined. Only in some cases, possible competitive reactions are also considered. Rarely paths of different spin multiplicities are compared, and sometimes the multiplicity of intermediate species along the reaction path is not indicated. The oxidation state of the metal is only explicitly analysed in a specific case,^[63] although in many cases it is assumed in the proposed catalytic cycle. In a few cases, the reaction of PS or SD is studied.

As already commented, the first computational study on the catalytic reduction of CO₂ was developed in 2015 by the group of Robert.^[96] They focused on the mechanisms of the competitive reactions of CO₂ to CO and HCOOH catalysed under visible light by two complexes, one of Co(II) and another of Fe(III) with a pentadentate N5-donor ligand (**dmpbop** = 2,13-dimethyl-3,6,9,12,18-pentaazabicyclo[12.3.1]-octadeca-1(18),2,12,14,16-pentaene) (**8** and **9** respectively, Scheme 3). The Co(II) complex was selective to the formation of CO both in photo- and electrocatalytic processes, whereas the Fe(III) complex produced HCOOH in an electrocatalytic system. Thus, a CO₂ saturated solution of **8** in MeCN/TEA with the photosensitiser **PS2**



Scheme 3. Mechanism of the CO₂ reduction reactions catalysed by **8** and **9** (**dmpbop** = 2,13-dimethyl-3,6,9,12,18-pentaazabicyclo[12.3.1]-octadeca-1(18),2,12,14,16-pentaene). Adapted from ref. [96] Copyright (2015), with permission from the American Chemical Society.

produced selectively CO (97%) with an average TOF of 21.9 h⁻¹ using TEA as SD. The CV studies identified the metal-centred reduction process leading to the [M'(dmpbop)]⁺ species and the reduction waves centred on the ligand [M'(dmpbop)]/[M'(dmpbop•-)]ⁿ⁻. The CV of the CO₂-saturated solution of the cobalt complex showed an increase of current at the level of the [Co(dmpbop)]/[Co(dmpbop•-)]⁻ process. The authors proposed that the excited PS, PS*, was efficiently quenched by the cobalt catalysts [Co(dmpbop)]²⁺, with a constant $k_{\text{quenching}} = 0.68 \times 10^{10} \text{ L mol}^{-1} \text{ s}^{-1}$ determined presumably by fluorescence quenching measurements.^[97] They proposed that the active species [Co(dmpbop•-)]⁻ is formed in a two-electron reduction process.

The computational studies were performed omitting, to simplify, the reactions of capture of electrons and protons. They focused on the transformations that undergo the intermediate in which COOH⁺ is coordinated to the catalyst since this is the key species that, when reduced, produces HCOO⁻ or CO and OH⁻. The reaction profiles obtained with the computational studies (collected in Figure 6) showed that in the case of the Co(II) complex the most favoured reaction (with lower barriers) corresponds to the formation of CO and OH⁻, while with the Fe(III) complex the barrier of formation of HCOO⁻ is lower, what explains the experimental observations. The mechanisms proposed for both cases are shown in Scheme 3. The authors argue that in the electron-rich Co^{II}-COOH species there is a strong back donation of electrons to the $\pi^* 2T_{1u}$ LUMO of CO₂ so that the C–O bond weakens and breaks easily. In the less electron-rich Fe^{III}-COOH intermediate, however, this back donation is weaker, and the cleavage of the C–O bond is slower which allows an isomerisation of the intermediate to occur, which dissociates from the catalyst producing the formate. The multiplicities considered are quintuplet in the case of the Fe complex and triplet in the case of that of Co.

The same year a work^[63] that focused on CO₂ reduction catalysed by [Co^{II}(dtabhp)]²⁺ (**dtabhp** = 2,12-dimethyl-3,7,11,17-tetraazabicyclo-[11.3.1]-heptadeca-1(17),2,11,13,15-pentaene, **10**, Figure 7)) used temporally resolved FT-IR spectroscopy for the detection and structural determination of intermediates in light-induced catalytic systems under operating conditions

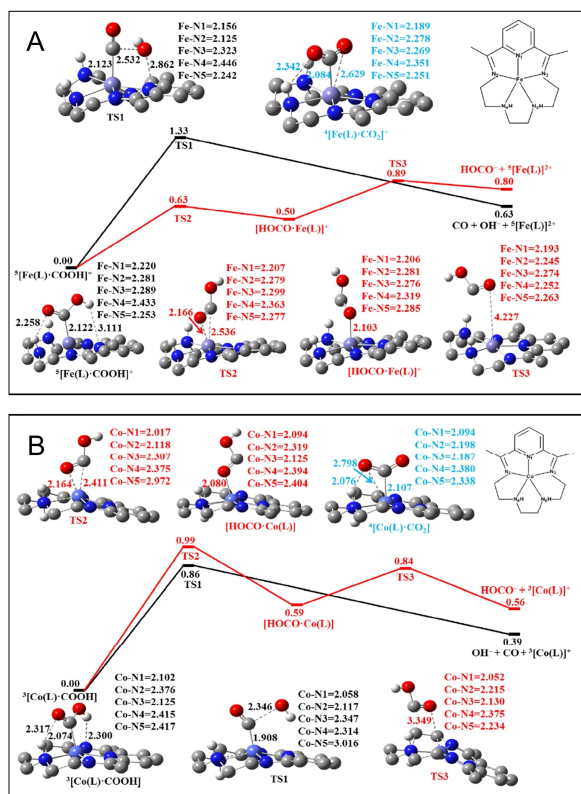


Figure 6. Potential energy profiles of the reaction pathways for the formation of CO + OH⁻ (black) and HOCO⁻ (red) catalysed by A) **9** [Fe((dmpbop))] and B) **8** [Co((dmpbop))] (dmpbop = 2,13-dimethyl-3,6,9,12,18-pentaazabicyclo[12.3.1]-octadeca-1(18),2,12,14,16-pentaene). Reproduced from ref. [96] Copyright (2015), with permission from the American Chemical Society.

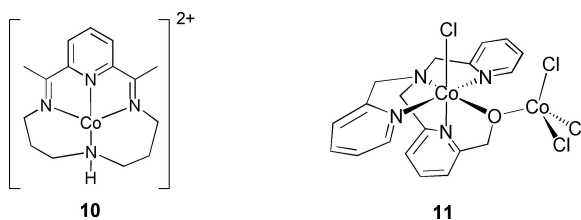


Figure 7. Left: Structure of **10** [Co^{II}(dtahbp)]²⁺. Adapted from ref. [63] Copyright (2015), with permission from the American Chemical Society. Right: Structure of **11** cis-[CoCl(μ-O-tpao)CoCl₃]. Adapted from ref. [48] (Copyright (2018), with permission from the Royal Society of Chemistry.

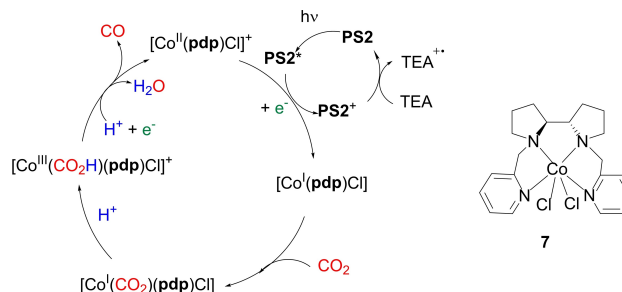
together with DFT computations. The authors studied the species formed using two different PS: **PS1**, which was known to reduce the complex [Co^{II}(dtahbp)]²⁺ to form H₂,^[103] and **PS2**, which reducing potential was expected to be enough to generate CO. In fact, when a solution of **10**, in wet acetonitrile saturated CO₂ solution was irradiated for 3 h with a laser (405 nm) in presence of **PS2** and TEA, CO was detected by FT-IR. However, in a similar irradiation experiment for 1 min the cobalt complex in the presence of **PS2** at 458 nm, no carbon monoxide was detected by FT-IR. A signal at 1670 cm⁻¹ was observed instead, which was attributed to the formation of a

carbon dioxide adduct [Co^{I+δ}(dtahbp)(CO₂)^{δ-1}]⁺. Experiments with labelled ¹³CO₂ confirmed this hypothesis and experiments with labelled C¹⁸O₂ allowed to identify acetaldehyde as the product of TEA oxidation by oxygen transfer from CO₂.

The nature of the Co–CO₂ interaction in the adduct was further studied by computational methods. By analysing localised bond orbitals, the oxidation state of the Co atom in the different species that can be formed along the proposed reaction mechanism was determined. It was shown that the tetra-N-donor ligand plays an important role by sharing a certain part of the charge of the reduced photocatalyst, which is transferred to CO₂ once it is coordinated, so the bond formed is stronger than in other possible species.^[63]

In 2016, a study^[62] of different complexes of the type cis-[Co(pdp)Cl₂] (pdp = 1,1'-bis(2-pyridinylmethyl)-2,2'-bipyridoline, **7**, Scheme 4) with different levels of catalytic activity in the reduction of CO₂ was published. It was suggested that the crucial characteristic of this system to favour the activation of CO₂ for its photo- and electroreduction was the availability of two *cis* coordination positions. Thus, **7** photochemically catalyses the reduction of CO₂ to CO with a TON of 368 using **PS2** and TEA as a sacrificial electron-donor for a time of 60 h with high selectivity to CO with respect to H₂ (95 %).

To understand the factors that determine this activity, the authors first calculated the spin density difference plots of the complexes between their initial and reduced state (Figure 8 and observed that in those that were active (C1 to C4 and TPA in Figure 8, as opposite to C5), there was a resonance structure between Cl–Co(II)–pdp and Cl–Co(III)–pdp^{•-} shown by the spin density localised on the ligands, due to the existence of ligands σ-donor and π-acceptors that delocalise the 1 electron charge and decrease the energy of the reduction barrier. They also calculate the profiles of the reaction paths for the production of CO and H₂ along with the singlet and triplet states of lower energy and proposed a reaction mechanism (Scheme 4). It identifies as an active species a pentacoordinate reduced complex [Co^I(pdp)Cl] that by its strong nucleophilic character induced by the basic ligands activates the CO₂ by coordination in an axial position to form [Co^I(CO₂)(pdp)Cl].^[46] This Co–CO₂ adduct can be detected in the CV studies by the anodic displacement towards positive values of the half-wave potential



Scheme 4. Proposed mechanism for CO₂ photoreduction with the catalyst **7** (cis-[Co(pdp)Cl₂]), pdp = 1,1'-bis(2-pyridinylmethyl)-2,2'-bipyridoline using **PS2** as a photosensitiser and triethylamine (TEA) as a sacrificial reducer (SD). Adapted from ref. [62] Copyright (2016), with permission from the Royal Society of Chemistry.

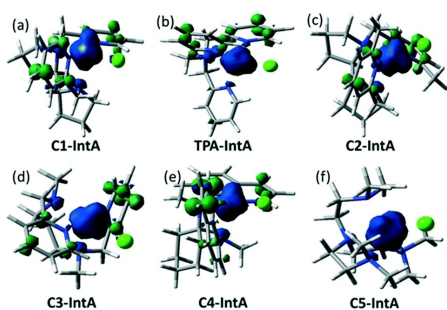


Figure 8. Spin-density difference plots of the α - and β -electron density for the reduction product of the type *cis*-[Co(**pdp**)Cl₂] (**pdp** = 1,1'-bis(2-pyridinylmethyl)-2,2'-bipyrrolidine Co(II) complexes studied in ref. [62]. Reproduced from ref. [62] Copyright (2016), with permission from the Royal Society of Chemistry.

($\epsilon_{1/2}$) corresponding to the Co^{III}/I reduction as a function of the CO₂ concentration with respect to the $E_{1/2}$ value measured when no CO₂ is present.^[104] This shift is produced when there is a fast reaction between the Co^I species and CO₂. The key of the mechanism would be the ease to undertake 2-electron exchanges between the Co(I)/Co(III) species. The protonation of the adduct to form [Co^{III}(CO₂H)(**pdp**)Cl] occurs with a very low energy barrier which has been attributed to the interaction by the hydrogen bond with the adjacent chloride. But the reactions to both CO and H₂ products are favourable so the results cannot explain the experimental observation of the selectivity of this catalyst towards the production of CO.

They also compared the profile for the reaction of CO production with different complexes finding that, in addition to the π -acceptor capacity, steric effects have a determining influence on the catalytic activity. These results allow them to highlight the importance of the *cis* architecture of the Cl ligands of these complexes for their catalytic efficacy.

The work of Zhu et al.^[48] studied the competitive pathways of CO, H₂ and HCOO⁻ formation in the photoreduction of CO₂ by a Co complex with a tris(2-pyridylmethyl)amine-type ligand with a -CH₂OH functionalised pyridine (**tpaoH** = 6-(bis(pyridin-2-ylmethyl)amino)methyl)pyridin-2-yl)methanol), a Cl⁻ ligand and an oxygen atom occupying a *cis* position to the coordinated chloride. The homogeneous photocatalytic system is formed by complex *cis*-[CoCl(μ -O-**tpao**)CoCl₂] (**11**, Figure 7) as a catalyst, **PS1** as a photosensitiser, and TEA as a sacrificial electron donor. The study was initially performed in saturated CH₃CN, with irradiation for 60 hours providing 80% CO selectivity. Interestingly, the variation of the CH₃CN/H₂O ratio leads to different results in activity and selectivity indicating a clear dependence on the solvent. In the water-rich solvent, the proton reduction predominates: while the presence of water promotes the formation of formic acid, in the solvent mixtures without water the formation of CO is favoured. The activity towards CO₂ was examined by cyclic voltammetry. During the reduction scan in a N₂ atmosphere, the complex exhibited two irreversible waves at $\epsilon = -1.50$ V and -1.83 V (vs. SCE), which were attributed to the Co(II)/Co(I) and Co(I)/Co(0) reduction events respectively, by comparison with the corresponding

values for the related unmodified tris(2-pyridylmethyl)amine (**tpa**) complex, [Co(**tpa**)Cl]⁺.^[105]

In the computational study, the authors determined four reaction paths, corresponding to the formation of CO (path A), HCOOH (paths B and C, with and without the binding of a SD molecule to the reactive complex) and H₂ (path D) (shown in Figure 9). The authors indicate that the dominant pathway will be that of CO formation in the absence of water, given that after the first common step, the barriers in path A are lower than those in paths B and C. But the barriers of path D are lower than those of path A, so this will be the dominant reaction if there are enough H⁺ in the environment. These results are in

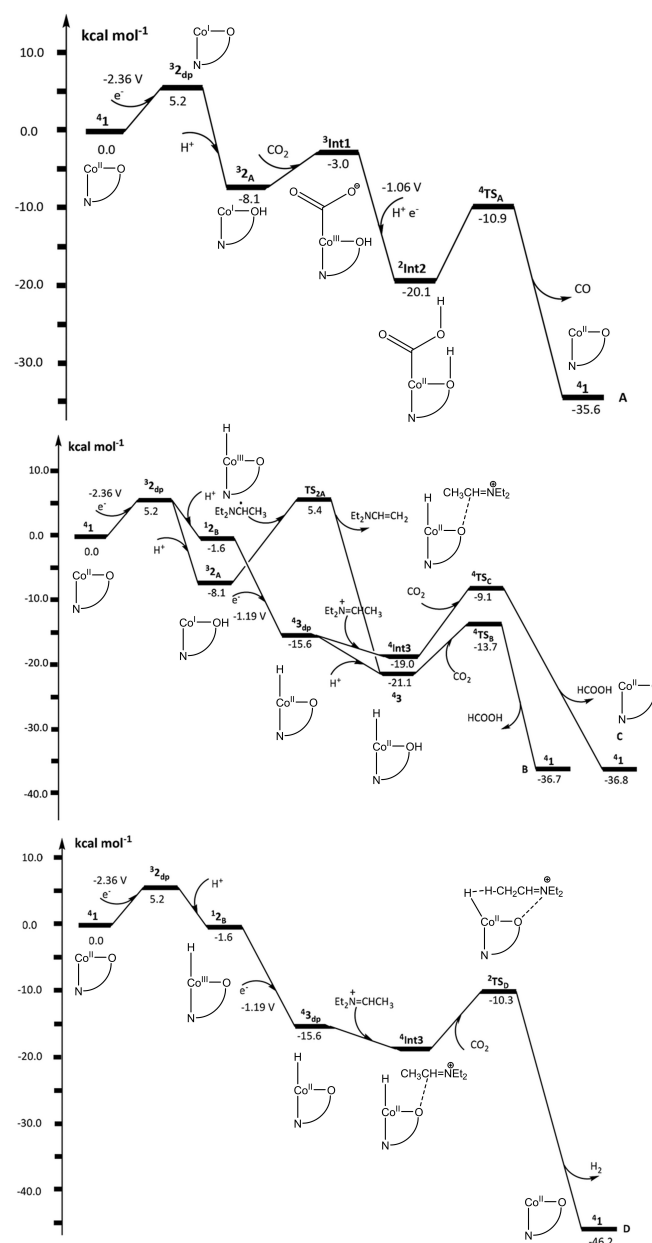
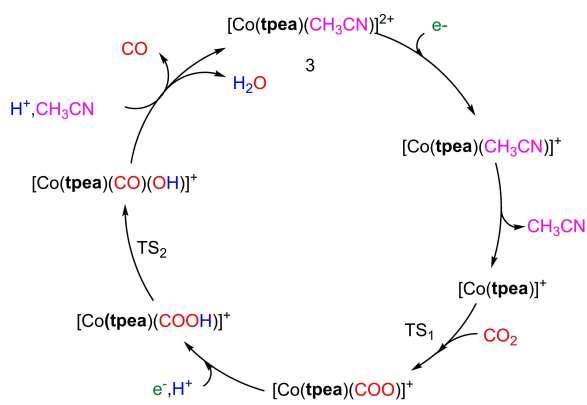


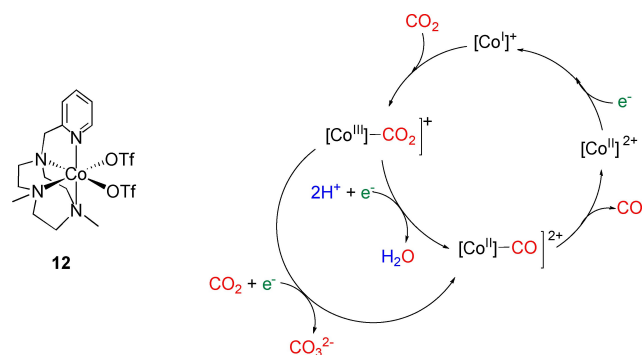
Figure 9. Gibbs free energy profiles of the reaction pathways of the reduction of CO₂ catalysed by **11** *cis*-[CoCl(μ -O-**tpao**)CoCl₂] to form CO (path A), HCOOH (paths B and C) and H₂ (path D). Reproduced from ref. [48] Copyright (2018), with permission from the Royal Society of Chemistry.

agreement with the experimental observations. The intermediates identified indicate that the presence of a O atom at the cis-coordination site of the catalyst is essential to stabilise some transition states of the reactions. This paper not only studies the mechanisms of possible CO₂ reduction reactions with different multiplicities of intermediate species (indicated by the superscripts of the species' acronyms in Figure 9), but also focuses on the possible consecutive reactions of oxidation and deprotonation of TEA that ends up producing diethyl-vinylamine.

The photocatalytic behaviour of the [Co(tpea)(CH₃CN)](ClO₄)₂ complex (**3**, Figure 5) in the CO₂ reduction was studied in detail in 2018 under different conditions.^[79] The activity for photocatalytic CO₂-to-CO conversion in a water-containing system achieved a TON of 44800 (10 h) with a 97% of CO selectivity. These results can be considered among the highest obtained for catalyst containing tripodal ligands. Another study of the same group modified complex **3** to incorporate the benzyl derivative ligand (**6**, Figure 5),^[44] and compared the efficiency of both catalysts. The results showed a decrease of the activity with complex **6** up to seven times under the same conditions. This higher efficiency of catalyst **3** is



Scheme 5. Proposed mechanism for the photoreduction of CO₂ with the catalyst [Co(tpea)(CH₃CN)](ClO₄)₂ (tpea = tris[2-(isopropylamino)ethyl]amine). Adapted from ref. [79].



Scheme 6. Catalytic cycle proposed for the electroreduction of CO₂ with complex **12** [Co(CF₃SO₃)₂(pmtcn)] (pmtcn = 1-[2-pyridylmethyl]-4,7-dimethyl-1,4,7-triazacyclononane). Adapted from ref. [46] Copyright (2015), with permission from the American Chemical Society.

attributed to the less steric hindrance of isopropyl groups in comparison with the benzyl groups in **6** which can facilitate the CO₂ binding to the catalytic centre as well as the electron transfer between the excited species.

The mechanism of the reaction catalysed by **3** (Scheme 5) was computationally corroborated. In view of the values of the reaction barriers obtained, it could not be established if there is a single determining stage of the reaction rate, since the values of the TS of the nucleophilic attack of CO₂ to the metal centre and that of the TS of the rupture of the C–OH bond are quite similar (17.2 kcal mol⁻¹ versus 13.8 kcal mol⁻¹), according to the authors' criterium.

The Lloret-Fillol group has also studied a complex of Co,^[46] in this case the [Co(pmtcn)(CF₃SO₃)₂] (pmtcn = 1-[2-pyridylmethyl]-4,7-dimethyl-1,4,7-triazacyclononane, **12**, Scheme 6). The detailed mechanistic study on the electrochemical CO₂-to-CO reduction developed in this work allows characterising intermediate Co species. In particular, it is relevant the use of "in situ" spectroelectrochemical techniques (UV-vis-SEC, FT-IR-SEC) and spectroscopic characterisation (¹H NMR and EXAFS) of intermediates generated by bulk electrolysis at the reduction peak of Co(II) to Co(I). The formation of new species at the first reduction event in a CO₂-saturated electrolyte was detected by FT-IR – SEC experiments in an IR optically transparent thin-layer electrochemical (OTTLE) cell providing the first in situ spectroscopic evidence for the formation of a Co(I)–CO at νCO = 1910 cm⁻¹, resulting from the electrochemical CO₂-to-CO reduction at the non-catalytic redox wave. This data confirms that the electrochemically generated Co(I) species is nucleophilic enough to bind the CO₂ molecule. Furthermore, the detection of the carbonyl species under these conditions shows that the C–O bond cleavage may take place at room temperature with no added protons in acetonitrile under a mild applied overpotential.

They also calculated the profiles of different possible pathways of the electrochemical reaction of CO₂ reduction to CO (subjected the system to different potentials).^[46] From these results, they infer a possible mechanism also for the photochemical reaction shown in Scheme 6 and draw valid conclusions for the two types of reaction, electro and photochemical. It is noteworthy that the singly occupied molecular orbital of the Co^{II/I/0}–CO complexes they obtained (shown in Figure 10) indicate that in the Co(II)–CO species there is no backdonation π from Co to CO, but it does exist in the species Co(I)–CO and Co(0)–CO. The species Co(I)–CO is very stable so, if it is formed,

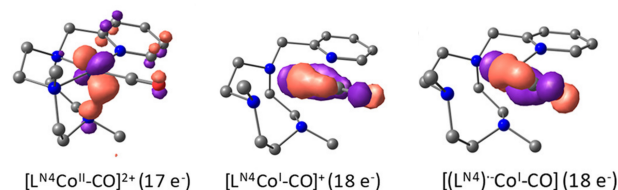


Figure 10. Singly occupied molecular orbital of Co^{II/I/0}–CO complexes (isovalue 0.07). Adapted from ref. [46] Copyright (2015), with permission from the American Chemical Society.

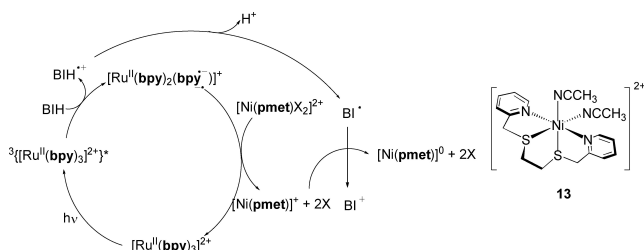
the release of CO is difficult, and the catalytic cycle is slowed down. This species is formed from the reduction of its precursor Co(II)–CO in a process that competes with the release of CO. In the electrochemical reaction, the reduction of Co(II) to Co(I) is faster than that of CO release, while in the photochemical reaction, under conditions of low concentrations of catalyst and PS, the ratio of the reaction rates of these competitive reactions is reversed, thus being the CO production more effective in photochemical conditions than by electrochemical processes. Another peculiarity of the results of this study is that they predict a coordination type $\eta^2\text{-C,O}$ for CO_2 with Co.

A paper by Angeles-Boza's group^[56] studied possible alternative pathways for the reduction of CO_2 by complex **1**, to elucidate the order in which reduction and protonation take place. In this paper it is proposed that the TEOA, in addition to acting as SD, assists in the protonation through the species TEOAH^+ which is formed by accepting a proton of the radical species $\text{TEOA}^{\bullet-}$, formed by oxidation of TEOA. Although it is generally assumed that reduction occurs before protonation, the low barrier found assuming the reverse order makes it impossible to reach an unequivocal conclusion in this case.

The development and mechanistic studies of Ni-based molecular complexes containing nitrogen ligands as photocatalytic catalysts in CO_2 reduction is particularly relevant since related Ni complexes have shown to be efficient in electrocatalytic CO_2 reduction. Nevertheless, there are only a few computational studies of Ni-based catalysts.

Recently Chen's group published a study^[80] of the CO_2 reduction catalysed by a Ni complex containing an uncommon tetradentate ligand of type S_2N_2 , the $[\text{Ni}(\text{pmet})\text{X}_2]^{2+}$ (**pmet** = bis(2-pyridylmethyl)-1,2-ethanedithiol, **X** = acetonitrile, **13**, Scheme 7). The experimental study^[66] was performed using a photocatalytic system formed by the Ni(II) complex, **PS2** as photosensitiser and BIH as an electron donor. This system shows a high TON over 700 after 55 h irradiation high CO selectivity of >99% and a quantum yield of 1.42% in the photocatalytic system. The Ni(II) complex **13** in its initial form is an even-electron metal complex which should be reduced to Ni(0).

The computational work begins with the determination of the ground state multiplicity of the catalyst, based on the



Scheme 7. Mechanisms of formation of catalytic Ni(I) and Ni(0) species proposed according to computational results from the joint action of catalyst **13** $[\text{Ni}(\text{pmet})\text{X}_2]^{2+}$ (**pmet** = bis(2-pyridylmethyl)-1,2-ethanedithiol, **X** = acetonitrile), photosensitiser $[\text{Ru}(\text{bpy})_3]^{2+}$ and sacrificial donor BIH. Adapted from ref. [80] Copyright (2020), with permission from the American Chemical Society.

relative energies of the triplet and singlet states and the comparison of the obtained geometries with the experimental X-ray diffraction structure previously reported.^[106] The results indicate that the $[\text{Ni}(\text{pmet})\text{X}_2]^{2+}$ ground state is a triplet. The oxidation and deprotonation reactions of the SD, BIH, with the intervention of the PS $[\text{Ru}(\text{bpy})_3]^{2+}$ (Scheme 7) were then calculated, finding that the photosensitiser follows a reducing deactivation mechanism. Its triplet excited state is quenched by BIH yielding $\text{BIH}^{\bullet+}$ and ${}^3\{[\text{Ru}(\text{bpy})_2(\text{bpy}^{\bullet-})]\}^+$. The last species reduces the catalyst to form $[\text{Ni}(\text{pmet})]^{+}$ with the loss of two acetonitrile molecules at the same time that $\text{BIH}^{\bullet+}$ transfer a proton to a water molecule affording a BI^{\bullet} radical. Given that this radical is a stronger reductant than ${}^3\{[\text{Ru}(\text{bpy})_2(\text{bpy}^{\bullet-})]\}^+$, the former species is the responsible for further reducing $[\text{Ni}(\text{pmet})]^{+}$, giving the active catalytic species $[\text{Ni}(\text{pmet})]^0$ in its triplet state.

$[\text{Ni}(\text{pmet})]^0$ can form an adduct with CO_2 of $\eta^2\text{-C,O}$ type that is then protonated, giving place to three possible intermediates. Only the two lowest energy ones, though, (**b-Int1** and **c-Int1** in Figure 11) are capable of giving place to CO_2 reduction reactions. The energy profiles of the possible pathways leading to CO and HCO_3^- (paths 1, 2, and 3) are shown in Figure 11.

$[\text{Ni}(\text{pmet})]^0$ can also be protonated in a facile and irreversible reaction, giving place to **h-Int1**. From this species, following reaction paths 4 and 5 (shown in Figure 11), H_2 and HCOOH can be obtained. Although the formation of CO is not the most favourable process, it is suggested that this is the dominant product due to the fact that the concentration of protons is lower than that of CO_2 in the medium.

The catalysts commented up to here contain a single metal centre, but there are also some studies focusing on complexes with several metal centres. The group led by Lu and Zhong published in 2017^[44] an experimental and computational study on the complex with two Co metal centres, the cryptane $[\text{Co}_2(\text{OH})(\text{cryp})](\text{ClO}_4)_3$ (**4**, Figure 5). The photocatalytic CO_2 reduction was performed in a CO_2 -saturated $\text{CH}_3\text{CN}/\text{H}_2\text{O}$ mixture, the Co complex, $[\text{Ru}(\text{phen})_3](\text{PF}_6)_2$ (**phen** = 1,10-phenanthroline) as photosensitiser, and TEOA as a sacrificial reductant. The results obtained from the photocatalytic experiments using as catalyst the dinuclear complex **4** show CO production together with trace amounts of formate detected in the liquid phase. In the absence of the dinuclear Co complex, CO production was not observed although small amounts of H_2 were detected. These results indicate that the dinuclear Co complex catalyses the CO_2 reduction to CO. The production of H_2 in the absence of catalyst can be ascribed to the fact that $[\text{Ru}(\text{phen})_3](\text{PF}_6)_2$ can act as both photosensitiser and catalyst for the photocatalytic reduction of H_2O into H_2 . Previous studies indicate that in this case and similar complexes (namely **PS1**) the active catalytic species is, in fact, formed by photodissociation of one of the ligands.^[107]

For comparison purposes, the mononuclear complex **6** was prepared following reported methods in the literature. The photochemical CO_2 reduction carried out under the same conditions provides for the mononuclear complex a TON value of 1600 (10 h) and a selectivity of 85% which are lower than

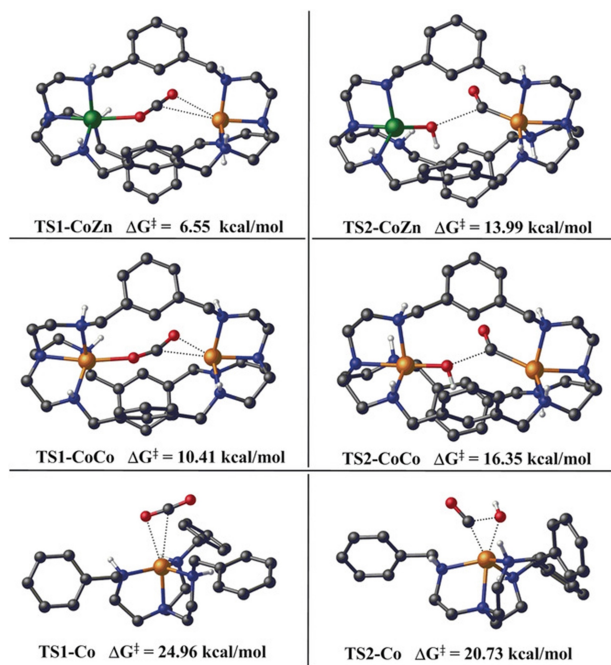
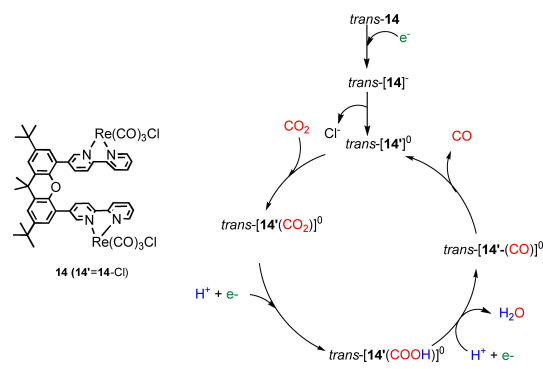


Figure 12. Structures and energies of the transition states of the reaction paths of CO₂ reduction to CO catalysed by the similar homodinuclear complex **4** (CoCo, Figure 5) and heterodinuclear complex **5** (CoZn, Figure 5). Reproduced from refs. [44, 47].

its mononuclear analogue. X-Ray diffraction shows a tetrahedral structure containing four six-coordinate Co(II) ions with the fifth central one forming a pentanuclear cluster and six **btz** ligands linking to five Co(II) ions. This complex offers the advantage of excellent solubility in the most common organic solvents. Photocatalytic CO₂ reduction was performed with **PS1** as a photosensitiser in MeCN and TEOA as sacrificial reductant. Reactivity reaches a TON of ~2748 and this reactivity could be maintained for more than 200 h showing the stability of this homogeneous molecular catalyst, although variable compositions of CO and H₂ were obtained for different reaction conditions.

The authors also computed reaction profiles for the reactions of the penta- and mononuclear complexes with the energies of the reaction intermediates (without calculations of the barriers of the different stages), from which they could not draw clear conclusions.^[92]

The most recent paper on this line focuses on a complex of the 5d metal Re, obtained binding two (**bpy**)Re(CO)₃Cl fragments by a xanthene link to maintain both metallic centres close together (**14**, Scheme 9).^[102] Opposite to the 2020 work by Shipp^[101] et al. where the dimerisation of a Re complex did not catalyse the CO₂ to CO reaction, **14** showed an enhancement factor of the catalytic activity of 45 relative to its monometallic counterpart. Photocatalytic CO₂ reduction experiments were performed in DMF solutions with either TEA or BIH as an electron donor. Carbon monoxide was the only gaseous product obtained in all experiments. The long-term stability



Scheme 9. Mechanism of the CO₂ reduction catalysed by **14** as proposed in the literature. Adapted from ref. [102] Copyright (2021), with permission from the American Chemical Society.

was higher with the bimetallic catalyst when using BIH as the electron donor.

The crucial species of the reaction of CO₂ to CO and its mechanism was studied with several experimental techniques (steady-state absorption and emission spectroscopy, time-correlated spectroscopy, nanosecond kinetic emission spectroscopy, cyclic voltammetry and others).

Computational studies elucidated which one of the possible *cis/trans* isomers and in/out conformers of catalyst **14** is most stable and corroborated the hypothesis regarding the reduction events proposed on the base of cyclic voltammetry experiments by optimising the geometry of the reduced complexes. The authors also analysed the frontier orbitals of the *trans*-**14** complex to interpret its excitations in the absorption spectra and obtained structural information by geometry optimisations of the possible catalytic intermediates of the reaction. The aim was not to calculate the reaction mechanism profile, but to corroborate the intermediates suggested by experimental measurement to be able to discern between the possible reaction paths: the binding of the CO₂ substrate to only one of the Re centres, singly or doubly reduced, or the cooperative activation of CO₂ by both singly reduced Re atoms. With the information collected, the authors suggest that in the photochemical reaction the CO₂ binds to a singly reduced Re centre and follows the mechanism shown in Scheme 9, while the other Re moiety functions as a photosensitiser to assist the first catalytically active metal atom.

In the same line of development of catalytic systems for CO₂ reduction of unifying photosensitised and catalyst, a work has been published recently^[98] in which a series of complexes are studied computationally seeking to displace their absorption bands to the visible zone to achieve a hybrid photocatalyst, being capable of coordinating CO₂ and at the same time absorbing in the visible area and promoting the reduction of the substrate. Based on previous experimental CO₂ photo-reduction studies^[108,109] this work considers the thiophene-based donor-acceptor-donor (D–A–D) oligomer substituted metal-porphyrins (**15**, Figure 13) with different 3d central metal-ions (M = Co, Ni, Cu, and Zn). This paper analyses computationally the spectra of the different complexes and their ability to

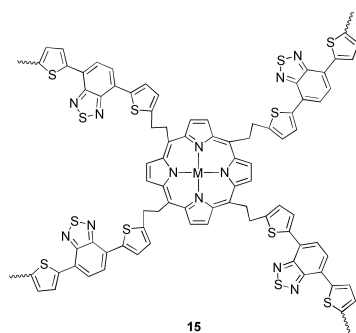


Figure 13. Structure of 15.^[98]

adsorb CO₂. These hybrid catalysts would adsorb CO₂ at the metal centre and harvest light at the D–A–D electron donor groups during the reduction process.

The optimised structures of photocatalysts of the four investigated 3d transition metal complexes exhibit good planarity which is important since it affects the photocatalysts' degree of conjugation that improves their catalytic performance. The results revealed that the mode of CO₂ adsorption over the catalyst active site depends on the type of central metal and that the most promising of the complexes is the one that incorporates Zn as metal centre.

This work opens an interesting line of research that would simplify and make more economical the photocatalytic reduction of CO₂, as long as non-precious metals should be used.

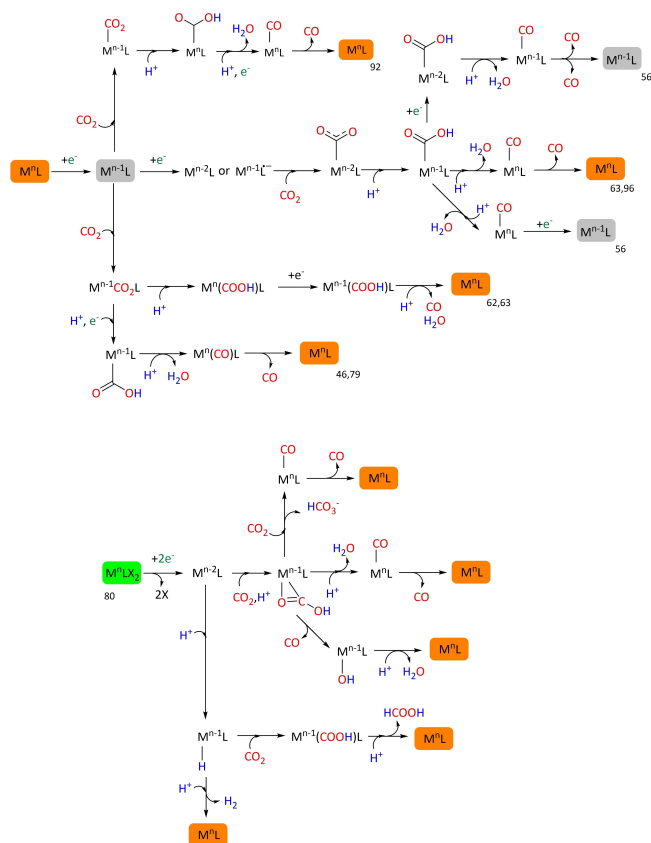
5. Conclusion and perspectives

The different mechanisms proposed in these works are compiled in a simplified way in Scheme 10 without including some other possible processes such as coordination / dissociation of ligands or solvent molecules if they do not explicitly intervene in the reaction, or cooperation of other species at some stage of the reaction. Scheme 10 shows the large number of alternative paths that the reaction of reduction of CO₂ to CO can follow and therefore the complexity of the process to be studied.

The panorama of the current state of development of catalyst systems for CO₂ photoreduction shows the achievements made so far and points to the aspects in which there is room for improvement, towards which mechanistic studies research should focus.

Selectivity is one of the key aspects that must be controlled. Although this aspect has been quite optimised in systems in organic solvents, the selectivity decreases drastically in most cases in the presence of water, due to the tendency to produce H₂, a reaction that in aqueous environments competes with the reduction of CO₂ to CO. It is therefore advisable to know the factors that can favour one or another reaction.

Another important point is the activity of the molecular systems. Although some catalysts with high TON and TOF values have already been proposed, the efficiency of catalysts is



Scheme 10. Different mechanisms proposed in the literature based on computational results.

in general low and should be improved. Quantum yield is in all cases very low (0.8–2%),^[28] so the effectiveness of photosensitisers has a large margin of improvement.

Many of the catalytic systems are coloured, so the opacity of the system is high. This ability to absorb light makes them inherently unstable under irradiation, so robustness is a feature that must be explicitly sought for.

Economical and simple catalytic systems must be developed to make feasible their integration into commonly used devices. In this sense, it is necessary to avoid the use of precious metals in both catalysts and photosensitisers. The first option is to replace them with abundant metals in both. For PSs, it would be a better option to replace them by organic compounds or even biocatalysts.

Another line of research looks for the integration of photosensitiser and catalyst to obtain better catalytic systems. Although there already are some examples where the same compound could absorb light, activate CO₂ and produce its reduction (like rhenium bipyridine systems^[49,50] or the family of iron complexes with modified tetraphenylporphyrins^[93]), these kinds of systems are scarce, so the room for improvement in this line is wide. There are, however, other possible strategies. One of them is the design of systems with tight electronic interactions between the catalysts and the PS. The strategy of integrating into the same molecule the complexes that

constitute the PS and catalytic units would not, in principle, simplify the synthesis nor make the catalyst more economical, but important progress is being made in the development of these supramolecular systems.^[111] In this case, the mechanistic studies from both, experimental and theoretical points of view, are specially challenging due to the possible existence of cooperative effects between all components of the catalytic systems.

Another option is the design of supported molecular catalysts, where the support can act as a light harvester^[112–117] and even as electron-donor.^[118,119] The synergy between catalyst and support can also provide some added advantages: the closeness between light harvester and catalytic units can improve the reaction yield and kinetics (faster charge transfer and more efficient charge separation) improving consequently the catalytic performance at the same time that the heterogenisation of the catalysts allows a more efficient and easier recycling procedure. Active research is also being developed in this line but theoretical studies are yet scarce due to the complexity of the systems.

A source of inspiration for the design of more efficient catalysts could be enzymes, given that some of them like carbon monoxide dehydrogenases (CODH) and formate dehydrogenases (FDH) are found to catalyse two-electron reduction of CO₂. Enzymes have evolved over billions of years to achieve high selectivity and performance in mild conditions using only abundant materials from the environment (Ni and Fe in the case of CODH and Mo or W in the case of FDH). Although their use at the industrial level (even at a small scale) presents severe drawbacks like the lack of robustness at operational conditions and the difficulty of obtention and purification in large amounts, if the mechanism of these metabolic processes is deeply understood, similar principles could be applied for the design of synthetic catalysts.^[20,120,121]

From the mechanistic point of view, the photocatalytic reduction of CO₂ is a complex process involving several steps of electron/proton transfer, CO₂ activation, C–O breaking bonds that can take place in different order to form the products. Computational studies have been useful to disclose the mechanism of photocatalytic reduction of CO₂ in different systems as they have allowed to determine the sequence of the different processes and to identify the key rate-determining steps, complementing the information obtained experimentally.

In fact, the elucidation of the reaction mechanism for these photocatalytic processes is not an easy task and the synergy between experimental and theoretical studies seems crucial to succeed in this endeavour. Nevertheless, there are still challenging questions to face in both approaches. From the computational point of view, although the increasing computational power of the methodologies allows to tackle medium size molecular systems with high accuracy, it is still difficult to study systems as complex as the ones involved in the photocatalytic reduction of CO₂. In most cases, it is necessary to use chemical models (i.e. to choose a portion of the system to be taken into account into the high-level computation) which are still very limited in comparison with the complexity of a real catalytic system. Despite the methods specifically designed to tackle

complexity (combination of quantum mechanics and molecular mechanics methods (QM/MM), solvent models...), it is impossible to reproduce accurately a system formed by millions of molecules of different types.

Another challenge is the unavoidable partial exploration of the potential energy surfaces (PES). Although chemical knowledge is very useful to narrow down the states (ground and excited states corresponding to different oxidation states) and the areas of the PES to be mapped, it can constitute a dangerous bias. Scheme 10 shows the large diversity of reaction paths found up to now for specific cases, but we must not discard other possibilities for other systems different from the ones studied here. To explore so many possibilities is still a big challenge for computational chemistry that will have to make use of massive calculations of machine learning algorithms. It would be desirable that a critical mass of systematic studies could allow us to understand the influence on the catalytic performance of factors such as the stereochemistry of the catalyst, the ligands' steric and electronic effects, the interactions among the various components of the catalytic system (substrate, Cat, PS, SD and even solvent), etcetera. We still have a long way to go.

From an experimental point of view, the challenges in mechanistic studies are the detection of the intermediate species with very short lifetimes in sequences of redox and hydrogen transfer processes with photoactivated species. The combination of spectroscopic and mass spectrometry techniques under photoelectrocatalytic conditions are necessary to identify not only the active species but also the deactivation paths.

In any case, it is necessary and seems crucial that experimental and computational approaches continue complementing each other to advance in the endeavour of obtaining efficient and cheap catalytic systems to be able to close the carbon cycle.

Acknowledgements

The authors are thankful to the Spanish Ministerio de Ciencia e Innovación and AEI/FEDER UE (PID2019-104427RB-I00 and PID2020-113187GB-I00), the Catalan Departament de Recerca i Universitats (2017 SGR 1472 and 2017 SGR 629) and Xarxa d'R + D + I en Química Computacional (XRQTC).

Conflict of Interest

The authors declare no conflict of interest.

Keywords: Carbon dioxide reduction · Density functional calculations · Molecular catalysts · Photocatalysis · Reaction mechanisms

[1] Robert Rapier, "Fossil Fuels Still Supply 84 Percent Of World Energy — And Other Eye Openers From BP's Annual Review," can be found

- under <https://www.forbes.com/sites/rpapier/2020/06/20/bp-review-new-highs-in-global-energy-consumption-and-carbon-emissions-in-2019/?sh=2f26c4ce66a1>, 2020.
- [2] IPCC, *Climate Change 2013. The Physical Science Basis*, 2013.
- [3] UN, *Report of the Secretary-General on the 2019 Climate Action Summit and the Way Forward in 2020*, 2019.
- [4] European Commission, *2050 Long-Term Strategy | Climate Action*, 2018.
- [5] European Union, *A Hydrogen Strategy for a Climate Neutral Europe The Path towards a European Hydrogen Eco-System Step by Step*, 2020.
- [6] International Energy Agency, *Achieving Net-Zero Emissions by 2050 – World Energy Outlook 2020 – Analysis – IEA*, 2020.
- [7] T. P. Senftle, E. A. Carter, *Acc. Chem. Res.* **2017**, *50*, 472–475.
- [8] K. M. K. Yu, I. Curcic, J. Gabriel, S. C. E. Tsang, *ChemSusChem* **2008**, *1*, 893–899.
- [9] S. Nanda, S. N. Reddy, S. K. Mitra, J. A. Kozinski, *Energy Sci. Eng.* **2016**, *4*, 99–122.
- [10] E. S. Sanz-Pérez, C. R. Murdock, S. A. Didas, C. W. Jones, *Chem. Rev.* **2016**, *116*, 11840–11876.
- [11] C. Bettenhausen, *C&EN News* **2021**, *99*, 28–35.
- [12] F. D. Rossini, R. S. Jessup, *J. Res. Natl. Bur. Stand. (1934)*. **1938**, *21*, 491.
- [13] D. G. Yu, L. N. He, *Green Chem.* **2021**, *23*, 3499–3501.
- [14] M. Aresta, A. Dibenedetto, A. Angelini, *J. CO₂ Util.* **2013**, *3–4*, 65–73.
- [15] M. Aresta, A. Dibenedetto, E. Quaranta, *J. Catal.* **2016**, *343*, 2–45.
- [16] L. Fan, C. Xia, F. Yang, J. Wang, H. Wang, Y. Lu, *Sci. Adv.* **2020**, *6*, eaay3111.
- [17] Q. Liu, L. Wu, R. Jackstell, M. Beller, *Nat. Commun.* **2015**, *6*, 5933.
- [18] Y. Tsuji, T. Fujihara, *Chem. Commun.* **2012**, *48*, 9956–9964.
- [19] C. Maeda, Y. Miyazaki, T. Ema, *Catal. Sci. Technol.* **2014**, *4*, 1482–1497.
- [20] A. M. Appel, J. E. Bercaw, A. B. Bocarsly, H. Dobbek, D. L. Dubois, M. Dupuis, J. G. Ferry, E. Fujita, R. Hille, P. J. A. Kenis, C. A. Kerfeld, R. H. Morris, C. H. F. Peden, A. R. Portis, S. W. Ragsdale, T. B. Rauchfuss, J. N. H. Reek, L. C. Seefeldt, R. K. Thauer, G. L. Waldrop, *Chem. Rev.* **2013**, *113*, 6621–6658.
- [21] I. Omae, *Coord. Chem. Rev.* **2012**, *256*, 1384–1405.
- [22] T. Sakakura, J.-C. Choi, H. Yasuda, *Chem. Rev.* **2007**, *107*, 2365–2387.
- [23] M. Aresta, A. Dibenedetto, A. Angelini, *Chem. Rev.* **2014**, *114*, 1709–1742.
- [24] J. Klankermayer, S. Wesselbaum, K. Beydoun, W. Leitner, *Angew. Chem. Int. Ed.* **2016**, *55*, 7296–7343; *Angew. Chem.* **2016**, *128*, 7416–7467.
- [25] M. Aresta, A. Dibenedetto, E. Quaranta, *Reaction Mechanisms in Carbon Dioxide Conversion* **2015**.
- [26] I. Castro-Rodríguez, H. Nakai, L. N. Zakharov, A. L. Rheingold, K. Meyer, *Science* **2004**, *305*, 1757–1759.
- [27] E. Fujita, C. Creutz, N. Sutin, D. J. Szalda, *J. Am. Chem. Soc.* **1988**, *110*, 4870–4871.
- [28] E. Boutin, L. Merakeb, B. Ma, B. Boudy, M. Wang, J. Bonin, E. Anxolabéhère-Mallart, M. Robert, *Chem. Soc. Rev.* **2020**, *49*, 5772–5809.
- [29] M. Schwartz, M. E. Vercauteren, A. F. Sammells, *J. Electrochem. Soc.* **1994**, *141*, 3119–3127.
- [30] M. E. Dry, *Catal. Today* **2002**, *71*, 227–241.
- [31] Q. Liu, L. Wu, R. Jackstell, M. Beller, *Nat. Commun.* **2015**, *6*, 1–15.
- [32] X. Duan, J. Xu, Z. Wei, J. Ma, S. Guo, S. Wang, H. Liu, S. Dou, *Adv. Mater.* **2017**, *29*, 1701784.
- [33] X. Liu, S. Inagaki, J. Gong, *Angew. Chem. Int. Ed.* **2016**, *55*, 14924–14950; *Angew. Chem.* **2016**, *128*, 15146–15174.
- [34] S. Nahar, M. Zain, A. Kadhum, H. Hasan, M. Hasan, *Materials (Basel)*. **2017**, *10*, 629.
- [35] J. Shi, Y. Jiang, Z. Jiang, X. Wang, X. Wang, S. Zhang, P. Han, C. Yang, *Chem. Soc. Rev.* **2015**, *44*, 5981–6000.
- [36] N. Long, J. Lee, K.-K. Koo, P. Luis, M. Lee, *Energies* **2017**, *10*, 473.
- [37] G. W. Crabtree, N. S. Lewis, *Phys. Today* **2007**, *60*, 37–42.
- [38] S. Zhu, D. Wang, *Adv. Energy Mater.* **2017**, *7*, 1700841.
- [39] A. Bachmeier, F. Armstrong, *Curr. Opin. Chem. Biol.* **2015**, *25*, 141–151.
- [40] M. Asadi, K. Kim, C. Liu, A. V. Addepalli, P. Abbasi, P. Yasaei, P. Phillips, A. Behranginia, J. M. Cerrato, R. Haasch, P. Zapol, B. Kumar, R. F. Klie, J. Abiade, L. A. Curtiss, A. Salehi-Khojin, *Science* **2016**, *353*, 467–470.
- [41] T. Kong, Y. Jiang, Y. Xiong, *Chem. Soc. Rev.* **2020**, *49*, 6579–6591.
- [42] K. E. Dalle, J. Warnan, J. J. Leung, B. Reuillard, I. S. Karmel, E. Reisner, *Chem. Rev.* **2019**, *119*, 2752–2875.
- [43] E. Fujita, *Coord. Chem. Rev.* **1999**, *185–186*, 373–384.
- [44] T. Ouyang, H. H. Huang, J. W. Wang, D. C. Zhong, T. B. Lu, *Angew. Chem. Int. Ed.* **2017**, *56*, 738–743; *Angew. Chem.* **2017**, *129*, 756–761.
- [45] J. W. Wang, H. H. Huang, J. K. Sun, T. Ouyang, D. C. Zhong, T. B. Lu, *ChemSusChem* **2018**, *11*, 1025–1031.
- [46] S. Fernández, F. Franco, C. Casadevall, V. Martin-Diaconescu, J. M. Luis, J. Lloret-Fillol, *J. Am. Chem. Soc.* **2020**, *142*, 120–133.
- [47] T. Ouyang, H.-J. Wang, H.-H. Huang, J.-W. Wang, S. Guo, W.-J. Liu, D.-C. Zhong, T.-B. Lu, *Angew. Chem. Int. Ed.* **2018**, *57*, 16480–16485; *Angew. Chem.* **2018**, *130*, 16718–16723.
- [48] C. Y. Zhu, Y. Q. Zhang, R. Z. Liao, W. Xia, J. C. Hu, J. Wu, H. Liu, F. Wang, *Dalton Trans.* **2018**, *47*, 13142–13150.
- [49] J. Hawecker, J.-M. Lehn, R. Ziessel, *J. Chem. Soc. Chem. Commun.* **1983**, 536–538.
- [50] J. Hawecker, J.-M. Lehn, R. Ziessel, *Helv. Chim. Acta* **1986**, *69*, 1990–2012.
- [51] X. Qiao, Q. Li, R. N. Schaugaard, B. W. Noffke, Y. Liu, D. Li, L. Liu, K. Raghavachari, L.-S. Li, *J. Am. Chem. Soc.* **2017**, *139*, 3934–3937.
- [52] T. Morimoto, T. Nakajima, S. Sawa, R. Nakanishi, D. Imori, O. Ishitani, *J. Am. Chem. Soc.* **2013**, *135*, 16825–16828.
- [53] Y. Kou, Y. Nabetani, D. Masui, T. Shimada, S. Takagi, H. Tachibana, H. Inoue, *J. Am. Chem. Soc.* **2014**, *136*, 6021–6030.
- [54] Y. Tamaki, D. Imori, T. Morimoto, K. Koike, O. Ishitani, *Dalton Trans.* **2016**, *45*, 14668–14677.
- [55] H. Takeda, K. Koike, H. Inoue, O. Ishitani, *J. Am. Chem. Soc.* **2008**, *130*, 2023–2031.
- [56] T. W. Schneider, M. Z. Ertem, J. T. Muckerman, A. M. Angeles-Boza, *ACS Catal.* **2016**, *6*, 5473–5481.
- [57] K. Kobayashi, T. Kikuchi, S. Kitagawa, K. Tanaka, *Angew. Chem. Int. Ed.* **2014**, *53*, 11813–11817; *Angew. Chem.* **2014**, *126*, 12007–12011.
- [58] Y. Kuramochi, M. Kamiya, H. Ishida, *Inorg. Chem.* **2014**, *53*, 3326–3332.
- [59] S. Sato, T. Morikawa, T. Kajino, O. Ishitani, *Angew. Chem. Int. Ed.* **2013**, *52*, 988–992; *Angew. Chem.* **2013**, *125*, 1022–1026.
- [60] J. Qiao, Y. Liu, F. Hong, J. Zhang, *Chem. Soc. Rev.* **2014**, *43*, 631–675.
- [61] C. Costentin, M. Robert, J.-M. Savéant, *Chem. Soc. Rev.* **2013**, *42*, 2423–2436.
- [62] F. Wang, B. Cao, W. P. To, C. W. Tse, K. Li, X. Y. Chang, C. Zang, S. L. F. Chan, C. M. Che, *Catal. Sci. Technol.* **2016**, *6*, 7408–7420.
- [63] M. Zhang, M. El-Roz, H. Frei, J. L. Mendoza-Cortes, M. Head-Gordon, D. C. Lacy, J. C. Peters, *J. Phys. Chem. C* **2015**, *119*, 4645–4654.
- [64] Z. Guo, S. Cheng, C. Cometto, E. Anxolabéhère-Mallart, S.-M. Ng, C.-C. Ko, G. Liu, L. Chen, M. Robert, T.-C. Lau, *J. Am. Chem. Soc.* **2016**, *138*, 9413–9416.
- [65] M. Liu, X. Wang, Y. Jiang, J. Sun, M. Arai, *Catal. Rev. Sci. Eng.* **2019**, *61*, 214–269.
- [66] D. Hong, Y. Tsukakoshi, H. Kotani, T. Ishizuka, T. Kojima, *J. Am. Chem. Soc.* **2017**, *139*, 6538–6541.
- [67] V. S. Thoi, N. Kornienko, C. G. Margarit, P. Yang, C. J. Chang, *J. Am. Chem. Soc.* **2013**, *135*, 14413–14424.
- [68] C. Herrero, A. Quaranta, S. El Ghachtouli, B. Vauzeilles, W. Leibl, A. Cukaaloo, *Phys. Chem. Chem. Phys.* **2014**, *16*, 12067–12072.
- [69] J.-W. Wang, W.-J. Liu, D.-C. Zhong, T.-B. Lu, *Coord. Chem. Rev.* **2019**, *378*, 237–261.
- [70] H. Rao, L. C. Schmidt, J. Bonin, M. Robert, *Nature* **2017**, *548*, 74–77.
- [71] P. G. Alsaheb, A. Rosas-Hernández, E. Barsch, H. Junge, R. Ludwig, M. Beller, *Catal. Sci. Technol.* **2016**, *6*, 3623–3630.
- [72] H. Takeda, K. Ohashi, A. Sekine, O. Ishitani, *J. Am. Chem. Soc.* **2016**, *138*, 4354–4357.
- [73] H. Rao, J. Bonin, M. Robert, *ChemSusChem* **2017**, *10*, 4447–4450.
- [74] P. L. Cheung, C. W. Machan, A. Y. S. Malkhasian, J. Agarwal, C. P. Kubiak, *Inorg. Chem.* **2016**, *55*, 3192–3198.
- [75] H. Takeda, H. Koizumi, K. Okamoto, O. Ishitani, *Chem. Commun.* **2014**, *50*, 1491–1493.
- [76] W. J. Liu, H. H. Huang, T. Ouyang, L. Jiang, D. C. Zhong, W. Zhang, T. B. Lu, *Chem. A Eur. J.* **2018**, *24*, 4503–4508.
- [77] Z. Guo, F. Yu, Y. Yang, C.-F. Leung, S.-M. Ng, C.-C. Ko, C. Cometto, T.-C. Lau, M. Robert, *ChemSusChem* **2017**, *10*, 4009–4013.
- [78] N. Elgrishi, M. B. Chambers, X. Wang, M. Fontecave, *Chem. Soc. Rev.* **2017**, *46*, 761–796.
- [79] D.-C. Liu, H.-H. Huang, J.-W. Wang, L. Jiang, D.-C. Zhong, T.-B. Lu, *ChemCatChem* **2018**, *10*, 3435–3440.
- [80] B. Zhang, S. Yang, X. Zheng, Y. W. Ju, B. Z. Chen, *Organometallics* **2020**, *39*, 1176–1186.
- [81] K. Kalyanasundaram, *Coord. Chem. Rev.* **1982**, *46*, 159–244.
- [82] Y. You, W. Nam, *Chem. Soc. Rev.* **2012**, *41*, 7061–7084.
- [83] C. K. Prier, D. A. Rankic, D. W. C. MacMillan, *Chem. Rev.* **2013**, *113*, 5322–5363.
- [84] E. Mejía, S.-P. Luo, M. Karnahl, A. Friedrich, S. Tschierlei, A.-E. Surkus, H. Junge, S. Gladioli, S. Lochbrunner, M. Beller, *Chem. A Eur. J.* **2013**, *19*, 15972–15978.

- [85] H. Takeda, Y. Monma, H. Sugiyama, H. Uekusa, O. Ishitani, *Front. Chem.* **2019**, *7*, 418.
- [86] H. Fei, M. D. Sampson, Y. Lee, C. P. Kubiak, S. M. Cohen, *Inorg. Chem.* **2015**, *54*, 6821–6828.
- [87] H. Takeda, C. Cometto, O. Ishitani, M. Robert, *ACS Catal.* **2017**, *7*, 70–88.
- [88] H. Uoyama, K. Goushi, K. Shizu, H. Nomura, C. Adachi, **2012**, DOI 10.1038/nature11687.
- [89] Y. Wang, X. W. Gao, J. Li, D. Chao, *Chem. Commun.* **2020**, *56*, 12170–12173.
- [90] Y. Wang, L. Chen, T. Liu, D. Chao, *Dalton Trans.* **2021**, *50*, 6273–6280.
- [91] T. Ogata, Y. Yamamoto, Y. Wada, K. Murakoshi, M. Kusaba, N. Nakashima, A. Ishida, S. Takamuku, S. Yanagida, *J. Phys. Chem.* **1995**, *99*, 11916–11922.
- [92] M. Sun, C. Wang, C. Y. Sun, M. Zhang, X. L. Wang, Z. M. Su, *J. Catal.* **2020**, *385*, 70–75.
- [93] J. Bonin, M. Chaussemier, M. Robert, M. Routier, *ChemCatChem* **2014**, *6*, 3200–3207.
- [94] H. Rao, J. Bonin, M. Robert, *Chem. Commun.* **2017**, *53*, 2830–2833.
- [95] C. Costentin, S. Drouet, G. Passard, M. Robert, J. M. Savéant, *J. Am. Chem. Soc.* **2013**, *135*, 9023–9031.
- [96] L. Chen, Z. Guo, X. G. Wei, C. Gallenkamp, J. Bonin, E. Anxolabéhère-Mallart, K. C. Lau, T. C. Lau, M. Robert, *J. Am. Chem. Soc.* **2015**, *137*, 10918–10921.
- [97] J. Bonin, M. Robert, M. Routier, *J. Am. Chem. Soc.* **2014**, *136*, 16768–16771.
- [98] A. Ostovan, N. Papior, M. Zahedi, A. Z. Moshfegh, *Phys. Chem. Chem. Phys.* **2020**, *22*, 23128–23140.
- [99] S. Grimme, J. Antony, S. Ehrlich, H. Krieg, *J. Chem. Phys.* **2010**, *132*, DOI 10.1063/1.3382344.
- [100] D. R. Case, A. Spear, A. F. Henwood, M. Nanao, S. Dampf, T. M. Korter, T. Gunnlaugsson, J. Zubieta, R. P. Doyle, *Dalton Trans.* **2021**, *50*, 3479–3486.
- [101] J. D. Shipp, H. Carson, S. J. P. Spall, S. C. Parker, D. Chekulaev, N. Jones, M. Y. Mel'nikov, C. C. Robertson, A. J. H. M. Meijer, J. A. Weinstein, *Dalton Trans.* **2020**, *49*, 4230–4243.
- [102] R. Giereth, P. Lang, E. McQueen, X. Meißner, B. Braun-Cula, C. Marchfelder, M. Obermeier, M. Schwalbe, S. Tschierlei, *ACS Catal.* **2021**, *11*, 390–403.
- [103] A. H. A. Tinnemans, T. P. M. Koster, D. H. M. W. Thewissen, A. Mackor, *Recl. des Trav. Chim. des Pays-Bas* **1984**, *103*, 288–295.
- [104] J. Schneider, H. Jia, J. T. Muckerman, E. Fujita, *Chem. Soc. Rev.* **2012**, *41*, 2036–2051.
- [105] S. L. F. Chan, T. L. Lam, C. Yang, S. C. Yan, N. M. Cheng, *Chem. Commun.* **2015**, *51*, 7799–7801.
- [106] B. Adhikary, S. Liu, C. R. Lucas, *Inorg. Chem.* **2002**, *32*, 5957–5962.
- [107] J. M. Lehn, R. Ziessel, *J. Organomet. Chem.* **1990**, *382*, 157–173.
- [108] N. Sadeghi, S. Sharifnia, M. Sheikh Arabi, *J. CO₂ Util.* **2016**, *16*, 450–457.
- [109] X. Li, J. Yu, M. Jaroniec, X. Chen, *Chem. Rev.* **2019**, *119*, 3962–4179.
- [110] D. C. Liu, H. J. Wang, J. W. Wang, D. C. Zhong, L. Jiang, T. B. Lu, *Chem. Commun.* **2018**, *54*, 11308–11311.
- [111] G. Li, D. Zhu, X. Wang, Z. Su, M. R. Bryce, *Chem. Soc. Rev.* **2020**, *49*, 765–838.
- [112] T. Jin, C. Liu, G. Li, *J. Coord. Chem.* **2016**, *69*, 1748–1758.
- [113] F. Fang, Y. Liu, X. Sun, C. Fu, Y. Prakash Bhoi, W. Xiong, W. Huang, *Appl. Surf. Sci.* **2021**, *564*, 150407.
- [114] P. Kumar, H. P. Mungse, S. Cordier, R. Boukherroub, O. P. Khatri, S. L. Jain, *Carbon* **2015**, *94*, 91–100.
- [115] A. Kumar, P. K. Prajapati, M. S. Aathira, A. Bansiwala, R. Boukherroub, S. L. Jain, *J. Colloid Interface Sci.* **2019**, *543*, 201–213.
- [116] A. Sharma, B. K. Lee, *Catal. Today* **2017**, *298*, 158–167.
- [117] S. Guo, H. Zhang, Y. Chen, Z. Liu, B. Yu, Y. Zhao, Z. Yang, B. Han, Z. Liu, *ACS Catal.* **2018**, *8*, 4576–4581.
- [118] K. D. Dubois, H. He, C. Liu, A. S. Vorushilov, G. Li, *J. Mol. Catal. A* **2012**, *363–364*, 208–213.
- [119] H. M. Sung-Suh, D. S. Kim, C. W. Lee, S. E. Park, *Appl. Organomet. Chem.* **2000**, *14*, 826–830.
- [120] T. W. Woolerton, S. Sheard, Y. S. Chaudhary, F. A. Armstrong, *Energy Environ. Sci.* **2012**, *5*, 7470–7490.
- [121] A. Bachmeier, F. Armstrong, *Curr. Opin. Chem. Biol.* **2015**, *25*, 141–151.

Manuscript received: November 12, 2021
 Revised manuscript received: March 18, 2022
 Accepted manuscript online: March 23, 2022